



Pergamon

Acta mater. 49 (2001) 4041–4054



www.elsevier.com/locate/actamat

CONCURRENT GROWTH AND COARSENING OF SPHERES

L. RATKE¹ and C. BECKERMANN^{2,†}

¹Institute for Space Simulation, German Aerospace Research Center, DLR, 51140 Cologne, Germany and

²Department of Mechanical Engineering, The University of Iowa, Iowa City, IA 52242-1527, USA

(Received 9 July 2001; accepted 16 July 2001)

Abstract—A theory is developed of concurrent growth and coarsening of a dispersion of spheres that accounts for the exchange of heat by diffusion among the spheres due to their curvature differences and between the spheres and the environment due to an externally imposed heat extraction rate. The results show that in concurrent growth and coarsening the average particle radius asymptotically increases with the cube root of time, which is the same behavior as in separate growth and coarsening. The growth rate constant increases linearly with the heat extraction rate, from the LSW value in pure coarsening to a value that is 1.89 times larger in concurrent growth and coarsening with a heat extraction rate that just prevents particles from disappearing due to coarsening interactions. For larger heat extraction rates, coarsening has no effect on the particle growth rate, because the distribution becomes mono-sized. © 2001 Acta Materialia Inc. Published by Elsevier Science Ltd. All rights reserved.

Keywords: Concurrent growth and coarsening; Diffusion; Microstructure; Theory & modeling

1. INTRODUCTION

Concurrent growth and coarsening (Ostwald ripening) of a dispersion of particles occurs in many phase transformation and precipitation processes. One important example is solidification. During most solidification processes a mushy zone develops consisting of a mixture of dendrites or other microscopically complex solid structures in the melt. As a first approximation, the solid can be viewed as a dispersion of particles of different sizes. Due to continual heat extraction, the particles grow as the mixture solidifies. At the same time, the mixture undergoes a coarsening process driven by the curvature of the particles. In coarsening, larger particles with a low interfacial curvature grow at the expense of smaller particles with a high curvature. Thus, the average particle size in the mixture increases during coarsening, as in growth due to heat extraction. However, smaller particles that would remelt and disappear due to coarsening alone may actually survive and grow if the heat extraction is dominant. Larger particles may increase in size at a higher rate than would be expected from the heat extraction rate alone, because coarsening adds to their growth rate. Overall, the con-

current growth and coarsening results in a complex evolution of the particle sizes and spacings in solidification processes that cannot be explained by available theories [1, 2].

In the past, growth and coarsening of a dispersion of particles have only been analyzed as separate processes [3–7]. Growth is generally caused by heat removal from or species addition to a system or by an imposed supercooling or supersaturation. It results in an increase in the sizes of all particles and an increase in the particle volume fraction in the system, but the particle number density remains constant (in the absence of nucleation or coalescence). Coarsening, on the other hand, is due to the dependence of the solubility or melting point of a substance on the interface curvature (Gibbs–Thomson effect) and is controlled by the exchange of heat or species among the particles. The average particle size increases and the system asymptotically approaches the equilibrium melting temperature or solubility. Since in pure coarsening the larger particles grow at the expense of the smaller particles, the particle number density decreases with time while the particle volume fraction in the system remains constant. Because of the different or even opposing influences of growth and coarsening on the evolution of the particle sizes, volume fraction and number density, the two effects are not simply additive. A new theory is needed that considers growth and coarsening simultaneously.

All classical theories of pure growth and of pure

† To whom all correspondence should be addressed. Fax: +1-319-335-5669.

E-mail address: becker@engineering.uiowa.edu (C. Beckermann)

coarsening are based on the idealization that the dispersion of particles can be analyzed as a single particle in an infinite medium, which corresponds to the limit of vanishing particle volume fraction. The statistics of growth or coarsening are then determined by solving a continuity equation for the size distribution function. In standard theories of particle growth a constant driving force, such as an imposed supersaturation or supercooling, leads to a parabolic growth law for the particle radius with time [3–5]. All classical coarsening theories replace the constant driving force by one that depends on the curvature dependent solubility or melting point of a single particle with respect to a statistically averaged background solubility or supercooling (LSW theory, [6, 7]). Coarsening then becomes self-similar and the average particle radius is predicted to increase with the cube root of time. This well-known coarsening law has been confirmed experimentally numerous times [8, 9]. Other growth and coarsening laws have been derived for particles located at grain boundaries or along dislocation lines, for particles in a convecting liquid, and for particles undergoing interface reactions of first or second order [9]. In all cases, growth or coarsening laws of the form $R^n \propto t$ or $\langle R \rangle^n \propto t$ are obtained for the evolution of the particle radius R or the average radius $\langle R \rangle$ with time t .

The present study attempts to develop a theory for concurrent growth and coarsening. For simplicity, the discussion is limited to a dispersion of stationary solid spheres of a pure substance in a motionless melt, such that growth and coarsening are controlled by heat diffusion only. The paper is structured as follows. In Section 2, expressions for the particle growth rates for growth at a constant supercooling, growth at a constant heat extraction rate and pure coarsening are derived. This is followed by a review of the statistics of growth of a dispersion of particles in Section 3. In Section 4, the case of concurrent coarsening and growth of a particle dispersion is analyzed by deriving the general growth equation and then solving the continuity equation for the evolution of the size distribution function. Three limiting cases are considered that allow for an analytical solution. In Section 5, the analytical results are verified and generalized by solving the governing set of equations numerically. The conclusions of the present study are drawn in Section 6.

2. GROWTH RATES FOR A SINGLE PARTICLE

2.1. Growth at constant supercooling

The growth of a single sphere of radius R in a supercooled melt is schematically illustrated in Fig. 1. Far away from the interface the melt is at a constant temperature T_∞ which is below the equilibrium melting temperature T_m .

Growth is assumed to proceed slowly enough that a stationary interface approximation holds [3]. The

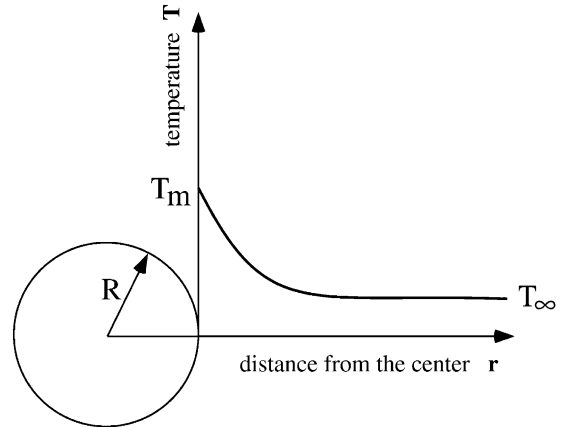


Fig. 1. Growth of a sphere of radius R into an infinite supercooled melt.

temperature distribution in the melt, $T(r)$, is then given by the solution of the steady, one-dimensional heat conduction equation in spherical coordinates:

$$\nabla^2 T = \frac{\partial^2 T}{\partial r^2} + \frac{2}{r} \frac{\partial T}{\partial r} = 0 \quad (1)$$

subject to the boundary conditions:

$$T(r \rightarrow \infty) = T_\infty \quad (2)$$

$$T(r = R) = T_m \quad (3)$$

The general solution of equation (1) is given by:

$$T(r) = A1 + \frac{B1}{r} \quad (4)$$

Evaluating the constants $A1$ and $B1$ using the boundary conditions, the complete solution is:

$$T(r) = T_\infty + T_m - T_\infty \frac{R}{r} \quad (5)$$

The growth rate of the sphere is obtained from a heat balance at the solid–liquid interface:

$$\rho L \frac{dV}{dt} = -k_L \left. \frac{\partial T}{\partial r} \right|_R A \quad (6)$$

where ρ is the density measured in kg/m^3 , L is the latent heat measured in J/kg , k_L is the liquid thermal conductivity measured in W/(Km) , and $A = 4\pi R^2$ and $V = 4\pi R^3/3$ are the surface area and volume of the

sphere, respectively. Taking the derivative of $T(r)$ in equation (5), the growth rate is given by:

$$\frac{dR}{dt} = \frac{k_L}{\rho L} \frac{T_m - T_\infty}{R} \quad (7)$$

For a constant supercooling $\Delta T = T_m - T_\infty$ and constant thermophysical properties, growth then proceeds in a parabolic manner as:

$$R^2 = R_0^2 + \frac{2k_L}{\rho L} \Delta T \cdot t = R_0^2 + K_T \cdot t \quad (8)$$

where K_T is the growth rate constant for the case of constant supercooling. Using thermophysical properties of succinonitrile (SCN) and a supercooling of $\Delta T = 0.5$ K, the growth rate constant is equal to $K_T \approx 2 \cdot 10^{-10}$ m²/s. This means that within 1 s a SCN particle would grow from a negligible initial size to 10 μ m in radius. In one day the particle would grow to a radius of approximately 4 mm.

2.2. Growth at a constant heat extraction rate

Another important growth mode is the case where not the supercooling, but the heat extraction rate Q_{single} measured in W at the boundary of a spherical volume V_{cv} of radius R_{cv} is kept constant. This situation is illustrated in Fig. 2.

Using again the stationary interface approximation, the general solution for the temperature field is given by equation (4). However, the boundary conditions become:

$$T(r = R) = T_i \quad (9)$$

$$-k_L \left. \frac{\partial T}{\partial r} \right|_{R_{cv}} = Q_{single} \quad (10)$$

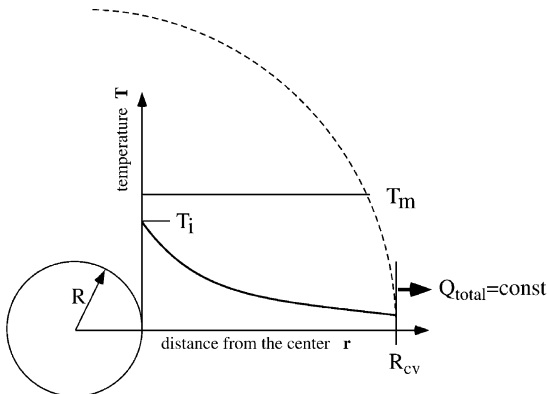


Fig. 2. Growth of a sphere of radius R in a melt cooled with a constant heat extraction rate.

where T_i is an interface temperature that could be but is not necessarily equal to the equilibrium melting temperature, T_m , and Q_{single} is the heat extraction rate corresponding to a single particle. For an arbitrary number N of spherical particles, the total heat extracted at the surface of the control volume, Q_{total} , is:

$$Q_{total} = N \cdot Q_{single} \text{ where } N = n \cdot V_{cv} = n \cdot \frac{4\pi}{3} R_{cv}^3 \quad (11)$$

and n is the number of particles per unit volume. Evaluating the constants in the general solution using the above boundary conditions, the temperature profile is given by:

$$T(r) = T_i - \frac{Q_{single}}{4\pi k_L} \left(\frac{1}{R} - \frac{1}{r} \right) \quad (12)$$

Using the interfacial heat balance, equation (6), the growth rate is:

$$\frac{dR}{dt} = \frac{Q_{single}}{\rho L} \frac{1}{4\pi R^2} \quad (13)$$

It is interesting to note that the growth rate does not depend on the interface temperature. Integrating the above equation yields that the particle radius grows with the cube root of time:

$$R^3 = R_0^3 + \frac{3Q_{single}}{4\pi \rho L} \cdot t = R_0^3 + K_Q \cdot t \quad (14)$$

where K_Q is the growth rate constant for the case of a constant heat extraction rate. Using again the thermophysical properties of SCN, the growth rate constant becomes:

$$K_Q^{SCN} = Q_{single} \cdot 6 \cdot 10^{-9} \text{ m}^3/(\text{sW}) \quad (15)$$

As is shown below, a reasonable heat extraction rate for a single particle is $Q_{single} = 0.1$ μ W. With that value the growth constant is equal to $K_Q^{SCN} = 6 \cdot 10^{-16}$ m³/s. Then, in 1 s a SCN particle would grow to a radius of 8.4 μ m from a negligible initial size. In one day the particle would grow to a radius of 373 μ m.

Defining the total heat extraction rate per unit volume as $q_{total} = Q_{total}/V_{cv} = Q_{single} \cdot n$, equation (13) can be rewritten as:

$$\frac{dR}{dt} = \frac{q_{total}}{n \rho L} \frac{1}{4\pi R^2} \quad (16)$$

Then, it is easy to see that the solid volume fraction f_s increases linearly with time:

$$f_s(t) = f_s(0) + \frac{q_{total}}{\rho L} t \quad (17)$$

According to this equation, it would require a constant heat extraction rate per unit volume of $q_{total} = 2.4 \cdot 10^4 \text{ W/m}^3$ to solidify a volume containing liquid SCN to 60 percent solid (corresponding to some packing of spheres) in 1000 s. With $Q_{single} = 0.1 \mu\text{W}$ from above, such a solidification rate could be achieved for a particle number density of $n = 2.4 \cdot 10^{11} \text{ m}^{-3}$. In these 1000 s, the spheres would grow to 84 μm in radius. This is a physically reasonable particle size (and, hence, particle number density), thus justifying the initial choice of Q_{single} as an example. Note that according to equation (8), growing a SCN particle to the same size in the same time would require a constant applied supercooling of only 0.02 K.

2.3. Pure coarsening

In pure coarsening of a dispersion of spheres, the radius evolution of a given sphere is driven not by an applied supercooling or heat extraction rate, but by the difference between its curvature dependent interface temperature, $T_i = T_m(R)$, and the average interface temperature, $\langle T_i \rangle$, of the whole ensemble of spheres of different radii. Thus, sensible heat is exchanged only among the spheres and not with the environment. As in all classical coarsening analyses, it is assumed that the solid spheres are far enough away from each other that a single sphere (dilute dispersion, zero volume fraction) approximation can be used. The temperature field around a sphere in the case of pure coarsening is illustrated in Fig. 3. In analogy with equation (7), the growth rate of a sphere in the pure coarsening case is given by:

$$\frac{dR}{dt} = \frac{k_L}{\rho L} \frac{T_i - \langle T_i \rangle}{R} \quad (18)$$

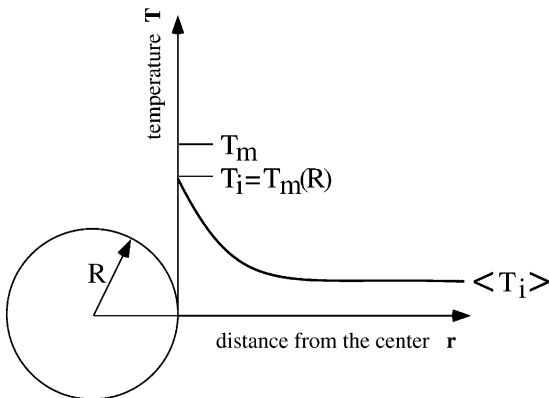


Fig. 3. Temperature field around a sphere undergoing pure coarsening.

The interface temperature is given by the Gibbs–Thomson equation:

$$T_i(R) = T_m \left(1 - \frac{\gamma}{\rho L R} \right) = T_m - 2\Gamma/R \quad (19)$$

where $\Gamma = \gamma T_m / (\rho L) = \gamma / \Delta s_f$ is the Gibbs–Thomson coefficient, Δs_f is the entropy of fusion, and γ is the solid–liquid interfacial energy. Similarly, the average interface temperature of the dispersion of spheres can be related to a so-called critical radius R^* by:

$$\langle T_i \rangle = T_m - \frac{2\Gamma}{R^*} \quad (20)$$

The exact definition of the critical radius in terms of the size distribution of spheres is provided in the next section. Physically, the melting temperature of spheres having the critical radius is exactly equal to the average interface temperature. Note that the average interface temperature and, hence, the critical radius change with time. Inserting the above equation into the expression for the growth rate, equation (18), and setting the interface temperature equal to the melting temperature of a sphere with radius R , equation (19), leads to:

$$\frac{dR}{dt} = \frac{k_L}{\rho L} \frac{2\Gamma}{R} \left(\frac{1}{R^*} - \frac{1}{R} \right) = \frac{2k_L\Gamma}{\rho L} \frac{1}{R^2} \left(\frac{R}{R^*} - 1 \right) \quad (21)$$

This equation for the growth rate in the case of pure coarsening cannot be solved easily because of the unknown time dependence of the critical radius. It is exactly the same growth rate equation as the one considered by LSW [6, 7]. Its solution requires a detailed consideration of the statistics of coarsening of a particle dispersion, which is reviewed in the next section.

For illustration purposes, it is useful to compare the growth rates in the case of pure coarsening with those in the pure growth cases obtained in the previous subsections. This can be accomplished by using the result from the LSW theory that the critical radius evolves with the cube root of time as:

$$(R^*)^3 - (R_0^*)^3 = \frac{8k_L\Gamma}{9\rho L} t = K_{LSW} t \quad (22)$$

where K_{LSW} is the LSW coarsening rate constant. The LSW analysis also shows that the critical and the average radius are identical. Using again the thermo-physical properties of SCN, the LSW rate constant is then equal to:

$$K_{LSW}^{SCN} = 2.7 \cdot 10^{-16} \text{ m}^3/\text{s} \quad (23)$$

Hence, in 1000 s an average SCN particle in a dispersion would grow to a radius of 65 μm from a negligible initial size. In one day the particle would grow to a radius of 300 μm . Note that the above value of the coarsening rate constant is very similar to the example value of the growth rate constant for the case of a constant heat extraction rate, equation (15) with $Q_{\text{single}} = 0.1 \mu\text{W}$. Whereas K_{LSW} is determined solely by thermophysical properties, K_Q depends on the imposed heat extraction rate and can be both smaller or larger than K_{LSW} . Nonetheless, the above example shows that similar particle growth rates in the cases of coarsening and constant heat extraction are possible and physically realistic. Also note that the above result for coarsening only applies to the average radius, and particles with other radii grow faster or shrink.

3. STATISTICS OF GROWTH

Before analyzing the case of concurrent growth and coarsening, it is necessary to consider the statistics of growth of a dispersion of particles. The statistics determine how an initial size distribution and the average particle radius change with time. The size distribution $f(r,t)dR$, defined as the number of particles with a radius in the interval $(R, R + dR)$ per unit volume, obeys the following continuity equation in size space:

$$\frac{\partial f}{\partial t} + \frac{\partial}{\partial R} \left(\frac{dR}{dt} f \right) = 0 \quad (24)$$

where dR/dt is the growth rate (i.e. interface velocity). With the knowledge of the size distribution function, its moments can be used to evaluate the following quantities:

$$\frac{1}{R^*} = \frac{1}{n} \int_0^{\infty} \frac{1}{R} f(R,t) dR \quad \text{critical radius} \quad (25)$$

$$n(t) = \int_0^{\infty} f(R,t) dR \quad \text{number density} \quad (26)$$

$$\langle R \rangle = \frac{1}{n} \int_0^{\infty} R f(R,t) dR \quad \text{average radius} \quad (27)$$

$$f_s(t) = \frac{4\pi}{3} \int_0^{\infty} R^3 f(R,t) dR \quad \text{volume fraction solid} \quad (28)$$

As is shown below, depending on the functional characteristics of dR/dt the fraction solid or the number density can be time independent.

Equation (24) can be solved quite generally for all growth laws of the type $dR/dt = K/R^n$. Defining the dimensionless radius r and time τ as:

$$r = R/R_{\text{ref}} \quad (29)$$

$$\tau = \frac{K}{R_{\text{ref}}^{n+1}} t \quad (30)$$

where R_{ref} is an arbitrary reference length scale (e.g. the capillary length or the initial mean radius), the growth law can be written as:

$$\frac{dr}{d\tau} = \psi(r) \quad (31)$$

In the above equation, $\psi(r) = 1/r^n$. Next, a new function $\zeta(r)$ is defined as:

$$\zeta(r) = - \int_0^r \frac{dr'}{\psi(r')} \quad (32)$$

and its inverse via the relation:

$$\zeta^{-1}(\zeta(r)) = 1 \quad (33)$$

Then, the solution of the initial value or Cauchy problem given by equation (24) for an arbitrary initial size distribution $f_0(r,0)$ can be written in dimensionless form as:

$$f(r,\tau) = \frac{\psi(\zeta^{-1}(\zeta(r) + \tau))}{\psi(r)} f_0(\zeta^{-1}(\zeta(r) + \tau)) \quad (34)$$

This general solution has been previously applied to growth at a constant supercooling [10, 11].

4. CONCURRENT GROWTH AND COARSENING OF A PARTICLE DISPERSION

In this section, concurrent coarsening and growth of a dispersion of spheres is analyzed by combining the growth rate expressions for the pure coarsening and pure growth cases derived in Section 2 and considering the statistics reviewed in Section 3. As mentioned in the Introduction, the two cases are not simply additive, and of particular interest are how the average radius, the solid volume fraction, the particle number density, and the size distribution function

evolve in the combined case. In this study, only the combination of coarsening with growth at a constant heat extraction rate is treated. In typical solidification processes, the heat extraction rate (and not the boundary temperature) is controlled or can be obtained from a simple heat flow analysis. Therefore, the case of growth at a constant heat extraction rate with concurrent coarsening is of greater practical interest. The case of concurrent coarsening and growth at a constant applied supercooling is most likely of less interest, because it is difficult to see how a constant supercooling could be maintained while the curvature dependent average interface temperature is continually changing. As noted above, in the case of a constant heat extraction rate the particle growth rate does not depend on the interface temperature. However, the reader is referred to the study of Beenakker and Ross [12] who analyzed coarsening of a precipitate for the case of an open system immersed in a reservoir of constant solute concentration, which is somewhat analogous to the case of a constant supercooling. They found that in the limit of an infinite system, the bulk of the system is screened from the reservoir by diffusive interactions among the particles.

In view of Section 2, the heat transfer rate for a single particle in the case of concurrent coarsening and growth at a constant heat extraction rate is given by:

$$Q_{single} = \frac{q_{total}}{n_0} + 4\pi k_L R(T_i - \langle T_i \rangle) \quad (35)$$

where n_0 is the initial number density of particles in the control volume. If the total heat extraction rate at the boundary of the control volume is zero, $q_{total} = 0$, pure coarsening results. Any difference between the interface temperature of a given particle and the average interface temperature of the dispersion adds or subtracts a heat flux from the external heat extraction rate. The general solution for the temperature profile around the particle is still given by equation (4). The constants are evaluated using the boundary conditions given by equations (9) and (10), but with Q_{single} in equation (10) replaced by the expression given by equation (35) above. Then:

$$T(r) = T_i - \frac{q_{total}}{n_0 \rho 4\pi k_L} \left(\frac{1}{R} - \frac{1}{r} \right) - (T_i - \langle T_i \rangle) R \left(\frac{1}{R} - \frac{1}{r} \right) \quad (36)$$

Using the interfacial heat balance and substituting the Gibbs–Thomson relation for the interface temperature, the following equation for the growth rate is obtained:

$$\frac{dR}{dt} = \frac{Q_{single}}{4\pi \rho L} \frac{1}{R^2} \quad (37)$$

$$= \frac{q_{total}}{n_0 4\pi \rho L} \frac{1}{R^2} + \frac{2k_L \Gamma}{\rho L} \frac{1}{R^2} \left(\frac{R}{R^*} - 1 \right)$$

The right hand side of the above equation is simply the sum of the growth rates given by equation (13) for pure growth at a constant heat extraction rate and equation (21) for pure coarsening. The dimensionless radius and time are defined, respectively, as:

$$r = R/\xi \quad (38)$$

$$\tau = \frac{\alpha_L}{\xi^2} t \quad (39)$$

where α_L is the thermal diffusivity of the liquid and ξ is an arbitrary length scale. If the length scale is taken to be $\xi = n_0^{-1/3}$, then in view of equation (26) the area under the normalized initial size distribution function $f(r, \tau = 0)$ is equal to unity. Equation (37) can now be rewritten as:

$$\frac{dr}{d\tau} = k_1 \frac{1}{r^2} + k_2 \frac{1}{r^2} \left(\frac{r}{r^*} - 1 \right) \quad (40)$$

where the two dimensionless prefactors are given by:

$$k_1 = \frac{q_{total}}{4\pi \rho L n_0 \alpha_L \xi} \quad (41)$$

$$k_2 = \frac{2k_L \Gamma}{\rho L \alpha_L \xi} \quad (42)$$

There are three special cases that are treated analytically below:

Case 1: k_1 is arbitrary and $k_2 = 0$, i.e. pure growth by external heat extraction.

Case 2: k_2 is arbitrary (although it would be fixed by thermophysical properties once ξ is specified) and $k_1 = 0$, i.e. pure coarsening.

Case 3: $k_1 = k_2 = k$; the heat extraction rate at the boundary of the control volume is of the same magnitude as the sensible heat exchange among the particles due to their curvature differences and fixed by $q_{total} = 8\pi \Gamma k_L n_0$ (then, $q_{single} = 8\pi \Gamma k_L = 0.3 \mu\text{W}$ for SCN). It will later be seen that this q_{total} is a critical heat extraction rate that just prevents particles from disappearing because of coarsening interactions.

4.1. Case 1

In the case of pure growth by external heat extraction, the dimensionless form of the growth law, equation (40), reduces to:

$$\frac{dr}{d\tau} = k_1 \frac{1}{r^2} \quad (43)$$

Inserting this growth rate into equations (32) and (33), the solution for the evolution of the size distribution function can be obtained from the general expression given by equation (34) as:

$$f_1(r, \tau) = \frac{r^2}{(r^3 - 3k_1\tau)^{2/3}} f_0((r^3 - 3k_1\tau)^{1/3}) \quad (44)$$

The subscript 1 on the size distribution function denotes that this solution corresponds to pure growth by external heat extraction, i.e. Case 1.

The zeroth moment gives the dimensionless particle number density as:

$$n(\tau) = \int_0^{\infty} \frac{r^3}{(r^3 - 3k_1\tau)^{2/3}} f_0((r^3 - 3k_1\tau)^{1/3}) dr \quad (45)$$

Introducing the transformation $\chi = (r^3 - 3k_1\tau)^{1/3}$, it is easy to show that the integral becomes:

$$n(\tau) = \int_0^{\infty} f_0(\chi) d\chi = n(\tau = 0) = 1 \quad (46)$$

The last equality holds if the distribution function is normalized. Hence, in pure growth by external heat extraction the particle number density is constant and equal to the initial value.

The asymptotic behaviour of the dimensionless average particle radius can be examined by evaluating the first moment. Using the same transformation as above, the average radius is given by:

$$\begin{aligned} \langle r \rangle &= \frac{1}{n} \int_0^{\infty} (\chi^3 + 3k_1\tau)^{1/3} f_0(\chi) d\chi \quad (47) \\ &= (3k_1\tau)^{1/3} \frac{1}{n} \int_0^{\infty} \left(1 + \frac{\chi^3}{3k_1\tau}\right)^{1/3} f_0(\chi) d\chi \end{aligned}$$

At long times, the second term in the integrand vanishes and the integral simply becomes the zeroth moment of the size distribution. Using equation (46), the average radius therefore evolves in the long-time limit with the cube root of time as:

$$\langle r \rangle = (3k_1)^{1/3} \cdot \tau^{1/3} \quad (48)$$

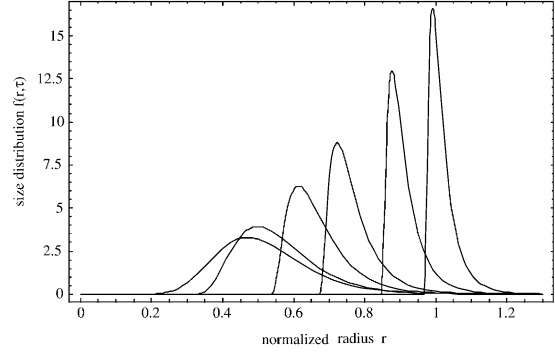


Fig. 4. Variation of the particle size distribution function with time for growth at a constant heat extraction rate (time increases from left to right as $\tau = 0, 0.01, 0.05, 0.1, 0.2, 0.3$).

Similarly, the solid volume fraction variation can be derived from the third moment as:

$$\begin{aligned} f_s(\tau) &= \frac{4\pi}{3} \int_0^{\infty} (\chi^3 + 3k_1\tau) f_0(\chi) d\chi \\ &= \frac{4\pi}{3} \int_0^{\infty} \chi^3 f_0(\chi) d\chi + 4\pi k_1 \tau \int_0^{\infty} f_0(\chi) d\chi \quad (49) \\ &= f_s(\tau = 0) + 4\pi k_1 n \tau \end{aligned}$$

where n in the last equality is constant and equal to unity if the initial size distribution is normalized. As expected, in the case of a constant heat extraction rate the solid volume fraction evolves linearly at all times.

In order to examine the behavior of the above solution in more detail, the following lognormal distribution is used as the initial particle size distribution function (note that $\chi = r$ for $\tau = 0$):

$$f_0(\chi) = \frac{1}{\sqrt{2\pi}\chi\sigma} \exp\left(-\frac{(\ln\chi - \langle \ln\chi_0 \rangle)^2}{2\sigma^2}\right) \quad (50)$$

Taking $k_1 = 1$, the evolution of this function, with the standard deviation $\sigma = 0.25$ and $\chi_0 = 0.5$, is shown in Fig. 4. The plot of the average radius in Fig. 5 rep-

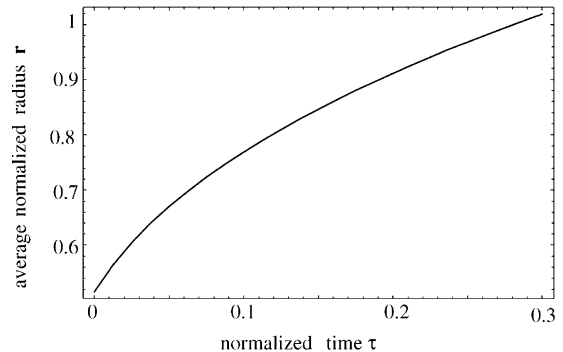


Fig. 5. Evolution of the average particle radius for growth at a constant heat extraction rate.

resents a curve fit of the first moments of the distribution functions shown in Fig. 4, and not just the long-time result given by equation (48). Corresponding to the increase of the average radius, the particle size distribution functions continually shift to the right in Fig. 4. Interestingly, the distributions become more narrow, indicating that the dispersion of particles approaches a state where the particle radius is increasingly uniform. This can be explained by the fact that the smaller particles in the dispersion grow more quickly than the larger ones for a constant heat extraction rate. After some time, the distribution is characterized by a relatively sharp lower cut-off very near the peak and a somewhat longer tail at larger radii. Since in pure growth by heat extraction the particle number density is constant, the area under the distributions in Fig. 4 is constant. Hence, as the the distribution becomes more narrow, the peak of the distribution function increases sharply.

4.2. Case 2

In the case of pure coarsening, $k_1 = 0$ and the general growth law given by equation (40) becomes:

$$\frac{dr}{d\tau} = k_2 \frac{1}{r^2} \left(\frac{r}{r^*} - 1 \right) \tag{51}$$

Since this equation is exactly the growth law analyzed by LSW [6, 7] in the low solid volume fraction limit, their results are only briefly reviewed here. By introducing the following coordinate transformation:

$$\rho = \frac{r}{r^*} \tag{52}$$

$$\theta = \ln \tau \tag{53}$$

the growth law can be rewritten as:

$$\frac{d\rho}{d\theta} = k_2 \frac{1}{(\rho^*)^2} \frac{d\rho^*}{d\theta} \left(\frac{\rho-1}{\rho^2} \right) - \rho \tag{54}$$

LSW showed that a stationary (self-similar) size distribution in ρ, θ -coordinates is obtained if the factor:

$$v = k_2 \frac{1}{(\rho^*)^2} \frac{d\rho^*}{d\theta} \tag{55}$$

is a constant. This constant is determined by the zeroth of $d\rho/d\theta$ and its first derivative with respect to ρ [6]. Performing the necessary calculations, LSW

obtained $v = 27/4$. Solving equation (55) for r^* and integrating gives:

$$(r^*)^3 = \frac{3k_2}{v} \tau = \frac{4}{9} k_2 \tau \tag{56}$$

LSW also showed that the critical radius and the average radius are identical. Hence, in terms of the variables used here, the average radius evolves in the long-time limit as:

$$\langle r \rangle = \left(\frac{4}{9} k_2 \right)^{1/3} \cdot \tau^{1/3} \tag{57}$$

which is simply a dimensionless version of equation (22) with the critical radius replaced by the average radius.

To further illustrate the results for pure coarsening, the evolutions of the size distribution function and the average radius are shown in Figs 6 and 7, respectively. These plots were obtained from a numerical solution of the leading system of equations using the initial size distribution given by equation (50) and setting $k_2 = 1$. As can be seen from Fig. 7, the expected cube root of time dependence of the average radius is only obtained after some time, and the initial average radius increase is much slower. Corresponding to the increase in the average radius, the size distribution functions in Fig. 6 continually shift to larger radii. Note that the size distribution is skewed about the maximum and consequently the peak does not coincide with the average radius. The area under the size distribution function decreases with time because the particle number density decreases hyperbolically with time. The decrease in the particle number density occurs by remelting of the smallest particles. By sca-

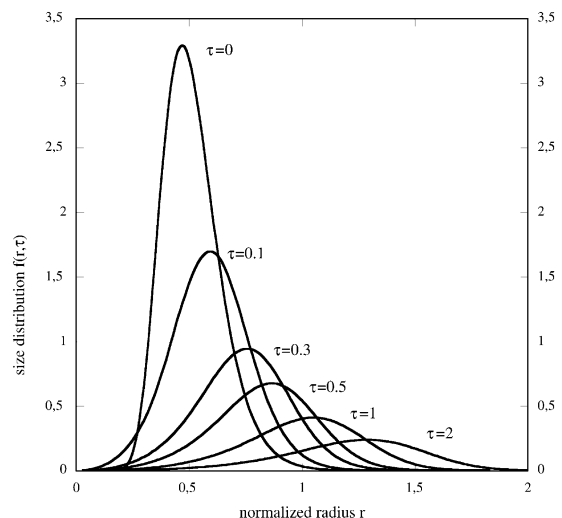


Fig. 6. Variation of the particle size distribution function with time in pure coarsening.

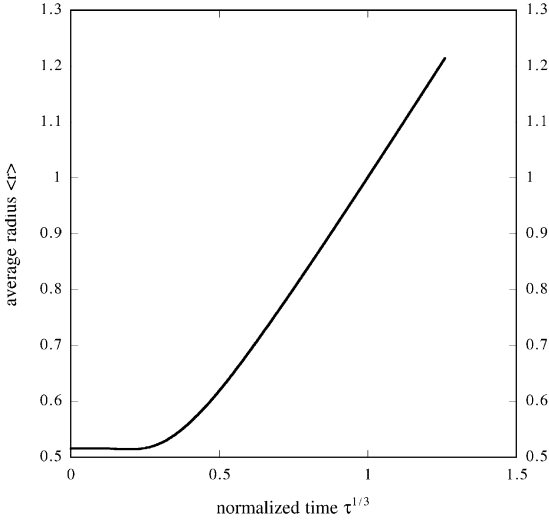


Fig. 7. Evolution of the average particle radius in pure coarsening.

ling the long-time size distribution functions with the average radius, the usual LSW distribution can be obtained. Such a scaled distribution function is time-invariant, implying that LSW-type coarsening is self-similar. The decrease in the particle number density coupled with the increase in the average radius result in a constant volume fraction solid in the case of pure coarsening.

4.3. Case 3

In the case of concurrent growth and coarsening with $k_1 = k_2 = k$, the general expression for the growth rate, equation (40), reduces to the following form:

$$\frac{dr}{d\tau} = k \frac{1}{r} \frac{1}{r^*(\tau)} \quad (58)$$

As in the case of pure coarsening, the solution of this equation requires the knowledge of the time dependence of the critical radius r^* . A simple analytical solution can still be obtained if only the long-time limit is considered. Since the average radius in both growth at a constant heat extraction rate and coarsening varies asymptotically with the cube root of time, it is reasonable to assume that the same time dependence holds in the combined case in the long-time limit, i.e.:

$$r^*(\tau) = a \cdot \tau^{1/3} \quad (59)$$

where a is a constant. This assumption is checked later through a numerical solution of the full system of equations. Insertion into equation (58) gives:

$$\frac{dr}{d\tau} = \frac{k}{ar \cdot \tau^{1/3}} \quad (60)$$

and after integration, the following cubic growth law for a single particle in the long-time limit is obtained:

$$r^3 = (3ka)^{3/2} \tau \quad (61)$$

Based on this single particle solution, the solid volume fraction grows linearly in time, since:

$$f_s = \frac{4\pi}{3} n R^3 = \frac{4\pi}{3} n \xi^3 (3ka)^{3/2} \tau \quad (62)$$

The constant a can be determined by realizing that the change in the solid volume fraction is only due to the external heat extraction rate and that the sensible heat exchange among the particles during coarsening does not change the solid fraction. For this purpose, equation (17) is rewritten in the long-time limit by introducing the dimensionless time as:

$$f_s = \frac{\xi^2 q_{total}}{\alpha_L \rho L} \tau \quad (63)$$

Comparing equations (62) and (63) gives:

$$a = \left(\frac{3q_{total}}{4\pi\alpha_L\rho L\xi n} \right)^{3/2} \frac{1}{3k} = (3k_1)^{2/3} \frac{1}{3k} = \left(\frac{1}{3k} \right)^{1/3} \quad (64)$$

since $k_1 = k_2 = k$.

In order to solve the statistical problem the continuity equation for the particle distribution function, equation (24), is recast in dimensionless form as:

$$\frac{\partial f_3}{\partial \tau} + \frac{\partial}{\partial r} \left(\frac{dr}{d\tau} f_3 \right) = 0 \quad (65)$$

where the subscript 3 on the distribution function denotes Case 3 where $k_1 = k_2 = k$. Inserting equation (60) into equation (65) gives:

$$\frac{\partial f_3}{\partial \tau} + \frac{\partial}{\partial r} \left(\frac{k}{ra \cdot \tau^{1/3}} f_3 \right) = 0 \quad (66)$$

or equivalently:

$$a \cdot \tau^{1/3} \frac{\partial f_3}{\partial t} + \frac{k}{r} \frac{\partial f_3}{\partial r} - \frac{k}{r^2} f_3 = 0 \quad (67)$$

Transforming time as:

$$\vartheta = 3/2a\tau^{2/3} \quad (68)$$

the continuity equation can be rewritten as:

$$\frac{\partial f_3}{\partial \vartheta} + \frac{k}{r} \frac{\partial f_3}{\partial r} - \frac{k}{r^2} f_3 = 0 \quad (69)$$

This equation has a simple solution for a given initial size distribution f_0 :

$$f_3(r, \vartheta) = \frac{r}{\sqrt{r^2 - 2k\vartheta}} f_0(\sqrt{r^2 - 2k\vartheta}) \quad (70)$$

or substituting equation (64) for a and transforming back to r, τ coordinates:

$$f_3(r, \tau) = \frac{r}{\sqrt{r^2 - (3k\tau)^{2/3}}} f_0(\sqrt{r^2 - (3k\tau)^{2/3}}) \quad (71)$$

Further insight into the nature of the solution can be gained by calculating the moments of the size distribution. The particle number density is given by the zeroth moment as:

$$n(\tau) = \int_{\sqrt[3]{3k\tau}}^{\infty} f_3(r, \tau) dr \quad (72)$$

$$= \int_{\sqrt[3]{3k\tau}}^{\infty} \frac{r}{\sqrt{r^2 - (3k\tau)^{2/3}}} f_0(\sqrt{r^2 - (3k\tau)^{2/3}}) dr$$

Transforming the integrand using $\chi = \sqrt{r^2 - (3k\tau)^{2/3}}$ leads to:

$$n(\tau) = \int_0^{\infty} f_0(\chi) d\chi = n(\tau = 0) = 1 \quad (73)$$

where the last equality holds if the distribution function is normalized. Thus, as in Case 1, the particle number density is constant in the case of concurrent growth and coarsening with $k_1 = k_2 = k$. This result can be explained by the fact that the death of the smallest particles occurring in pure coarsening is exactly prevented by their growth due to external heat extraction. In other words, the heat extraction rate given by $q_{total} = 8\pi\Gamma k_l n_0$ for $k_1 = k_2$ represents a critical heat extraction rate that just prevents particles from disappearing because of coarsening interactions.

The average radius is obtained from the first moment of the size distribution as:

$$\langle r \rangle = \frac{1}{n} \int_{\sqrt[3]{3k\tau}}^{\infty} \frac{r^2}{\sqrt{r^2 - (3k\tau)^{2/3}}} f_0(\sqrt{r^2 - (3k\tau)^{2/3}}) dr \quad (74)$$

Using the same transformation as above yields:

$$\langle r \rangle = \frac{1}{n} \int_0^{\infty} \sqrt{\chi^2 + (3k\tau)^{2/3}} f_0(\chi) d\chi \quad (75)$$

$$= (3k\tau)^{1/3} \frac{1}{n} \int_0^{\infty} \sqrt{1 + \frac{\chi^2}{(3k\tau)^{2/3}}} f_0(\chi) d\chi$$

Noting that the second term in the square root becomes negligibly small at long times and using equation (73) leads to the following asymptotic result:

$$\langle r \rangle = (3k)^{1/3} \tau^{1/3} \quad (76)$$

Hence, after some time the average particle radius grows with the cube root of time. Note that this solution is the same as the result obtained for the radius of a single particle, equation (61). However, at short times the average and single particle radii evolve differently.

The volume fraction solid is obtained by evaluating the third moment of the size distribution as:

$$f_s(\tau) = \frac{4\pi}{3} \int_{\sqrt[3]{3k\tau}}^{\infty} r^3 f_3(r, \tau) dr$$

$$= \frac{4\pi}{3} \int_{\sqrt[3]{3k\tau}}^{\infty} \frac{r^4}{\sqrt{r^2 - (3k\tau)^{2/3}}} f_0(\sqrt{r^2 - (3k\tau)^{2/3}}) dr \quad (77)$$

$$= 4\pi k \tau \int_0^{\infty} \left(1 + \frac{\chi^2}{(3k\tau)^{2/3}}\right)^{3/2} f_0(\chi) d\chi$$

At long times, the solution is given by:

$$f_s(\tau) = 4\pi k n \tau \quad (78)$$

where n is constant and equal to unity if the initial size distribution is normalized. Thus the volume fraction solid grows asymptotically linear in time.

The evolution of the particle size distribution given by equation (71) for Case 3 is shown in Fig. 8, taking equation (50) as the initial distribution and setting $k = 1$. The corresponding time variation of the average radius, obtained from a fit of the first moments, is shown in Fig. 9. The distributions appear qualitatively similar to the ones for growth at a constant heat extraction rate (Case 1), Fig. 4. With increasing time, they become more narrow with a sharp lower cut-off very near the peak, while the area under the distributions is constant. Note that the size distributions in

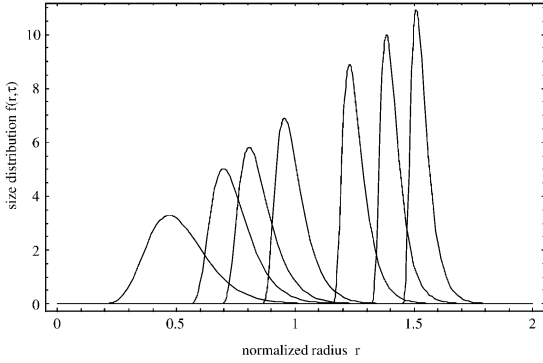


Fig. 8. Variation of the particle size distribution function with time for concurrent coarsening and growth at a constant heat extraction rate with $k_1 = k_2 = k = 1$ (time increases from left to right as $\tau = 0, 0.05, 0.1, 0.2, 0.5, 0.75, 1$).

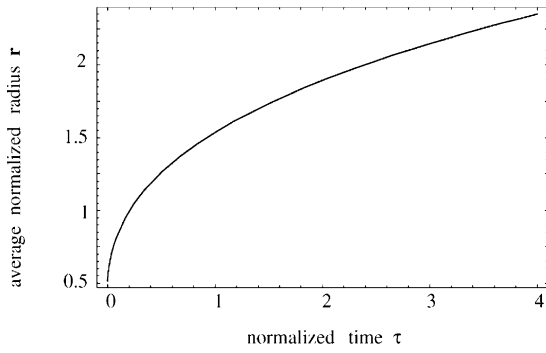


Fig. 9. Evolution of the average particle radius for concurrent coarsening and growth at a constant heat extraction rate with $k_1 = k_2 = k = 1$.

Case 1 [as given by equation (44)] and Case 3 [as given by equation (71)] are different.

4.4. Summary of long-time growth laws

In the previous subsections, analytical solutions are derived for three special cases of the general problem defined by the set of equations (24), (25), and (40). Analytical solutions for all values of k_1 and k_2 cannot be obtained. There is an analytical solution for the case of $0 < k_1 < k_2$, derivable using the LSW technique, which is omitted here.

The analytical solutions provide the following relations for the time dependence of the average radius in the long-time limit:

$$\langle r \rangle = (3k_1)^{1/3} \tau^{1/3} \text{ heat extraction, } k_2 = 0 \quad \text{Case 1:} \quad (79)$$

$$\langle r \rangle = (4k_2/9)^{1/3} \tau^{1/3} \text{ coarsening, } k_1 = 0 \quad \text{Case 2:} \quad (80)$$

$$\langle r \rangle = (3k)^{1/3} \tau^{1/3} \text{ concurrent, } k_1 = k_2 = k \quad \text{Case 3:} \quad (81)$$

Since in Case 3 $k_1 = k_2 = k$, it can be compared directly with the LSW result of Case 2. Denoting the rate constants according to $\langle r \rangle = K_j \tau^{1/3}$, with $j = 1, 2, 3$ denoting the three cases, the ratio of the rate constants for Cases 2 and 3 is given by $K_3/K_2 = (27/4)^{1/3} \approx 1.89$. Thus, concurrent growth and coarsening with $k_1 = k_2 = k$ proceeds 1.89 times faster than coarsening alone. Formally, Case 1 and Case 3 do not differ with respect to the rate constant. However, in Case 3 the rate constant is fixed by the condition $k_1 = k_2 = k$, whereas in pure growth k_1 is a variable determined by the imposed external heat extraction rate. The fact that Cases 1 and 3 are formally identical implies that if the external heat extraction rate in Case 1 is equal to $q_{total} = 8\pi\Gamma k_l n_0$, the growth rate is the same as in concurrent growth and coarsening, Case 3. In other words, coarsening has no effect on the long-time particle growth rate if the external heat extraction rate is equal to the critical heat extraction rate that just prevents particles from disappearing because of coarsening interactions. This interesting result is generalized and discussed in more detail in the next section.

In order to illustrate the above results more clearly, the three long-time growth laws given by equations (79), (80), and (81) are plotted in Fig. 10. In this figure, $k_2 = 1$ for Cases 2 and 3 and $k_1 = 3k_2$ for Case 1, implying that the external heat extraction rate is three times larger than the critical heat extraction rate that prevents particles from disappearing due to coarsening.

5. NUMERICAL SOLUTIONS FOR CONCURRENT GROWTH AND COARSENING

Since the analytical solution for concurrent growth and coarsening is limited to long times and $k_1 = k_2 = k$, the governing set of equations given by equations (24), (25) and (40), subject to the initial size distribution given by equation (50), was solved numerically for more general values of k_1 and k_2 using the technique described by Abbruzzese [13].

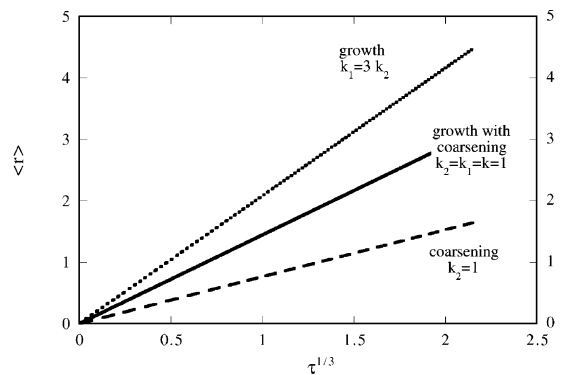


Fig. 10. Long-time evolution of the average particle radius for pure coarsening (with $k_2 = 1$), pure growth at a constant heat extraction rate (with $k_1 = 3k_2$), and concurrent growth and coarsening (with $k_1 = k_2 = k$).

This was also done to check if the analytically predicted long-time behavior based on the heuristic ansatz for the time dependence of the critical radius given by equation (59) is correct.

Numerical results for the evolution of the average particle radius are shown in Fig. 11 for various combinations of k_1 and k_2 . As expected, the slopes of the various curves reach a constant value after some time, implying that in each case the long-time average radius evolution is proportional to the cube root of time. The curve with the smallest slope is for the case of pure coarsening ($k_2 = 1$ and $k_1 = 0$). With increasing k_1 (keeping $k_2 = 1$) the slopes increase, since the addition of external heat extraction accelerates the particle growth over pure coarsening. The uppermost curve in Fig. 11 corresponds to concurrent growth and coarsening with $k_1 = k_2 = 1$, where the long-time growth rate is 1.89 times larger than the growth rate in pure coarsening. Interestingly, for $k_1 = 1$ the same curve is obtained for all $1 \geq k_2 \geq 0$. Therefore, coarsening has no effect on the particle growth rate for $k_1 \geq k_2$ or, equivalently, for $q_{total} \geq 8\pi\Gamma k_1 n_0$. Although not shown in the figure, this result is true not only for $k_1 = 1$ but for all values of k_1 , as long as $k_1 \geq k_2$ [note that the actual values of k_1 and k_2 depend on the choice of the length scale ξ in equations (41) and (42)]. Thus, the present numerical results generalize the analytical finding of the previous section, that the growth rate is formally the same for Cases 1 and 3, to all $k_1 \geq k_2$. The fact that coarsening does not affect the long-time particle growth rate if $k_1 \geq k_2$ can be explained by noting from Fig. 8 (for $k_2 = k_1$) that the size distribution becomes increasingly narrow at long times. Consequently, the particles ultimately become mono-sized and coarsening has no effect on the growth rate. For $k_1 < k_2$, on the other hand, coarsening does enhance the particle growth rate because the size distribution remains of a finite width even at long

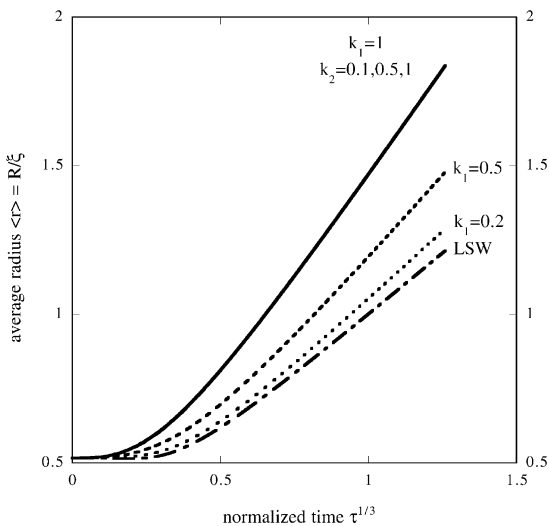


Fig. 11. Numerical results for the evolution of the average particle radius for various combinations of k_1 and k_2 ($k_2 = 1$ unless otherwise noted).

times and there continues to be sensible heat exchange among the particles.

The variation of the growth rate constant, defined as the long-time slope of the average radius variation with the cube root of time, with the dimensionless external heat extraction rate, k_1 , is shown in Fig. 12. The solid and open circles are obtained from the numerical results by measuring the long-time slopes of the curves shown in Fig. 11. These growth rate constants correspond to cases where coarsening is present, taking $k_2 = 1$. For the limiting cases of $k_1 = 0$ and $k_1 = 1$, the numerical results are compared to the analytical rate constants (open squares) given by equations (80) and (81), respectively. The analytical rate constants are $(4/9)^{1/3} \approx 0.763$ for $k_1 = 0$ and $(3)^{1/3} \approx 1.44$ for $k_1 = 1$. Overall, the numerical and analytical results are in satisfactory agreement for these two limiting cases, thus verifying the heuristic ansatz for the time dependence of the critical radius given by equation (59). The two numerical results shown at $k_1 = 1$ (solid and open circle) indicate that better agreement can be obtained if in the numerical calculations the time step is decreased and the time is increased (open circle). It has been observed previously that the long-time limit in coarsening systems is difficult to achieve numerically [14].

The numerical results indicate that the growth rate constant varies in an approximately linear fashion between $k_1 = 0$ and $k_1 = 1$ in the presence of coarsening ($k_2 = 1$). This variation with k_1 is represented by the dashed line in Fig. 12. For comparison, the corresponding variation for the case of no coarsening ($k_2 = 0$), given by equation (79), is included in Fig. 12 as a solid line. It can be seen that the rate constant without coarsening (solid line) increases in a nonlin-

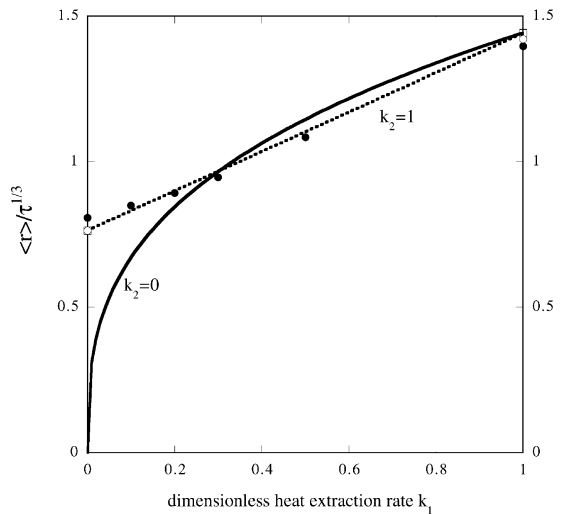


Fig. 12. Variation of the growth rate constant with k_1 and comparison of numerical (solid and open circles) and analytical (open squares) results for $k_2 = 1$. The dashed line represents the approximately linear variation of the growth rate constant between $0 < k_1 < 1$. The solid line corresponds to the case of no coarsening ($k_2 = 0$).

ear fashion from zero at $k_1 = 0$, and asymptotically approaches the dashed line for concurrent coarsening and growth at a constant heat extraction rate as k_1 increases to unity. Already at $k_1 = 0.2$ the two rate constants with and without coarsening are within approximately 6 percent, indicating that the effect of coarsening on the particle growth rate diminishes at relatively small external heat extraction rates. This comparison also shows that the dashed linear line cannot be accurate, because as drawn the rate constants for concurrent coarsening and growth are slightly below the values for pure growth at intermediate and larger $k_1 < 1$. In reality, the rate constants for the concurrent case can be expected to be always above those for pure growth. However, in the absence of more accurate numerical results the linear variation represented by the dashed line approximates the actual rate constants for concurrent coarsening and growth reasonably well. In accordance with the previous discussion, the rate constants for concurrent coarsening and growth for any $k_1 \geq k_2$ ($= 1$ in Fig. 12) are the same as for pure growth at a constant heat extraction rate ($k_2 = 0$, solid line).

Numerical results for the normalized particle number density evolution are shown in Fig. 13 for various combinations of k_1 and k_2 . As long as the external heat extraction rate is smaller than the critical heat extraction rate, i.e. $k_1 < k_2$, the particle number density decreases with time, with the strongest decrease observed in pure coarsening. Already at $k_1 = 0.5$ (with $k_2 = 1$), the decrease is very small. As soon as $k_1 = k_2$, the particle number density becomes a constant, and this is true for all $k_1 \geq k_2$. Hence, as with the particle growth rate, coarsening has no effect on the particle number density for $k_1 \geq k_2$ or, equivalently, for $q_{total} \geq 8\pi\Gamma k_L n_0$. To summarize, in pure coarsening ($k_1 = 0$) and for all $k_1 < k_2$ the particle

number density decreases, but for $k_1 \geq k_2$ the number density is constant.

6. CONCLUSIONS

Concurrent coarsening and growth by external heat extraction of a dispersion of solid spheres of a pure substance in their melt is analyzed. Coarsening and growth have different or even opposing influences on the evolution of a microstructure. Smaller particles that would remelt and disappear due to coarsening alone may actually survive and grow if the heat extraction is dominant. Larger particles may increase in size at a higher rate than would be expected from the heat extraction rate alone, because coarsening adds to their growth rate. Hence, the two effects are not simply additive.

It is found that in both pure coarsening and pure growth by external heat extraction, the radius of a single sphere increases with the cube root of time. Using these growth laws, a statistical analysis for a dispersion of spheres is performed. Analytical results are obtained for the limiting cases of pure coarsening ($k_1 = 0$), pure growth by external heat extraction ($k_2 = 0$), and concurrent coarsening and growth with $q_{total} = 8\pi\Gamma k_L n_0$ (or $k_1 = k_2$). From the analytical expressions for the evolution of the size distribution function, the average radius, the particle number density, and the volume fraction solid, as well as from supplementary numerical results, the following general conclusions can be drawn:

1. In all cases, the average radius increases in the long-time limit with the cube root of time. The growth rate constant for concurrent coarsening and growth with an external heat extraction rate that just prevents particles from disappearing due to coarsening interactions ($q_{total} = 8\pi\Gamma k_L n_0$ or $k_1 = k_2$) is 1.89 times larger than for pure coarsening ($k_1 = 0$). When the heat extraction rate is smaller ($k_1 < k_2$), the rate constant increases in an approximately linear fashion between $0 < k_1 < k_2$. When the heat extraction rate is larger ($k_1 \geq k_2$), the rate constant in the concurrent case is the same as in pure growth, implying that coarsening has no effect on the average particle growth rate.
2. Different size distribution functions are obtained in pure coarsening, pure growth by external heat extraction, and the concurrent case. In pure coarsening (LSW case) as well as for any $0 < k_1 < k_2$, the distribution function becomes in the long-time limit self-similar. For any $k_1 \geq k_2$, however, the distribution function becomes increasingly more narrow, indicating that the spheres approach a monosized distribution. This explains the fact that coarsening has no effect on the growth rate in the long-time limit if $k_1 \geq k_2$.
3. The particle number density in pure coarsening as well as for any $0 < k_1 < k_2$ decreases with time, whereas for any $k_1 \geq k_2$ the number density is con-

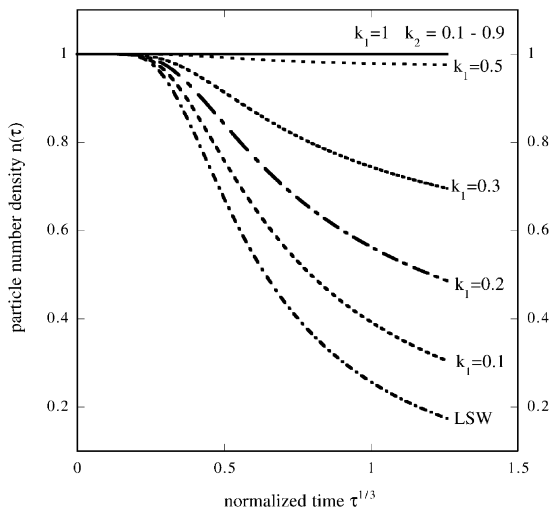


Fig. 13. Numerical results for the evolution of the normalized particle number density for various combinations of k_1 and k_2 ($k_2 = 1$ unless otherwise noted).

stant. Hence, k_2 can be identified as a critical dimensionless heat extraction rate for coarsening that just prevents particles from disappearing because of coarsening interactions.

4. The volume fraction solid is constant in the pure coarsening case. In the presence of a constant external heat extraction rate ($k_1 > 0$), the volume fraction increases, as expected, linearly in time. The rate constant is determined by the external heat extraction rate only, and this is true even for $0 < k_1 < k_2$ when coarsening still affects the particle growth rate and the number density.

The results presented here for pure growth ($k_2 = 0$) and for $k_1 \geq k_2$ are valid for finite volume fractions solid. However, the results for $k_1 < k_2$ apply only in the limit of vanishing volume fractions solid, even though the solid fraction increases with time when $k_1 > 0$. It is well known that in pure coarsening the evolution of a particle size distribution depends on the solid fraction [1]. Since the effect of coarsening becomes negligibly small as k_1 approaches k_2 , the critical heat extraction rate given by $k_1 = k_2$ can be expected to be independent of the volume fraction solid. Nonetheless, it would be interesting to extend the present analysis for $k_1 < k_2$ to the case of finite solid fractions.

It would also be interesting to compare the present results to experimental measurements. Unfortunately, no suitable experimental data are presently available for pure substances. An important extension of the present work would be the consideration of concurrent growth and coarsening for an alloy, which may provide insight into the evolution of the microstructure during alloy solidification processes. Even though coarsening in more concentrated alloys can be expected to be dominated by solute diffusion due to

the large value of the Lewis number [15], simultaneous heat removal still causes concurrent growth. Voorhees [15] only considered an adiabatic system in analyzing coarsening of a binary alloy solid-liquid mixture. Another interesting situation to consider would be concurrent melting and coarsening.

Acknowledgements—This work was conducted while the first author (LR) was on a sabbatical leave at The University of Iowa. The second author (CB) acknowledges the support by NASA under Contract No. NCC8-94.

REFERENCES

1. Marsh, S. P. and Glicksman, M. E., *Met. Trans.*, 1996, **27A**, 557.
2. Li, Q. and Beckermann, C., *Acta mater.*, 1999, **47**, 2345.
3. Aaron, H. B. and Kotler, G. R., *Met. Trans.*, 1971, **2**, 393.
4. Martin, J. W. and Dougherty, R. D., *Stability of Microstructures in Metallic Systems*. Cambridge University Press, Cambridge, UK, 1980.
5. Christian, J. W., *The Theory of Phase Transformations in Metals and Alloys*, 2nd ed. Pergamon Press, Oxford, UK, 1975.
6. Lifshitz, I. M. and Slyozov, V. V., *J. Phys. Chem. Solids*, 1961, **19**, 35.
7. Wagner, C., *Z. Elektrochemie*, 1961, **65**, 581.
8. Fischmeister, H. and Grimvall, G., in *Sintering and Related Phenomena*, ed. G. C. Kuczynski. Plenum Press, New York, 1973, p. 119.
9. Ratke, L., in *Progress in Astronautics and Aeronautics*, Vol. 130, ed. J. N. Koster and R. L. Sani. AIAA, Washington, DC, 1990.
10. Ratke, L., *Habilitation Thesis*, University of Stuttgart, Germany, 1988.
11. Latham, J., *Rep. Prog. Phys.*, 1969, **32**, 69.
12. Beenakker, C. W. J. and Ross, J., *J. Chem. Phys.*, 1985, **83**, 4710.
13. Abbruzzese, G., *Acta metall.*, 1985, **33**, 1329.
14. Alkemper, J., Snyder, V. and Voorhees, P. W., *Phys. Rev. Lett.*, 1999, **82**, 2725.
15. Voorhees, P. W., *Met. Trans.*, 1990, **21A**, 27.